A4 CAI COMPOSITION: DIVALENT ELEMENT PARTITIONING AND CATHODOLUMINESCENCE

A4.1 Anorthite and Melt compositions for Synthetic CAI Composition 224SAM

Anorthite-melt partitioning of divalent elements MgO, CaO, SrO, and BaO was also studied in the CMAST system based on the synthetic CAI-like composition 224 (Simon et al., 1994), which has been shown to readily crystallize anorthite under experimental conditions. Materials were prepared according to the procedures described in Miller et al. (2003) except that the starting material was also doped with 750 ppm Eu, which was present in concentrations just barely above detection limits. Since experiments were performed at ambient air oxygen fugacity, most (but not necessarily all) of the Eu would likely be trivalent and not relevant to divalent element partitioning systematics. Thus Eu contents of 224SAM21 phases were not analyzed.

Table A4.1. Glass and anorthite compositions for 224SAM run products analyzed by EMP. Glass uncertainty reported as standard error of the mean and anorthite error is 1 σ standard deviation.

Wt. %	224SAM1 Fused Glass n = 5	224SAM21 Glass n = 20	224SAM21 Anorthite n = 20
SiO_2	44.6 (2)	45.02 (5)	43.3 (2)
TiO_2	1.76 (6)	2.01 (2)	0.05 (3)
Al_2O_3	20.05 (6)	16.14 (2)	35.8 (2)
Eu_2O_3	0.09 (3)	na	na
MgO	3.86 (3)	4.760 (9)	0.27 (4)
CaO	28.03 (2)	29.68 (3)	19.9 (1)
SrO	0.07 (1)	0.07 (1)	0.08 (3)
BaO	1.35 (3)	1.65 (3)	0.36 (9)
Na_2O	0.035 (4)	0.025 (2)	0.027 (9)
	99.78	99.36	99.79

na = not analyzed

Electron microprobe conditions and standards are the same as those presented in Section 2.2.4 for low (25 nA) beam current analyses. Compositions (wt. %) of the fused starting material (run 224SAM1) and coexisting anorthite and glass in the controlled cooling experiment 224SAM21 are given in Table A4.1. Table A6.1 lists run conditions for these experiments.

Table A4.2. Modeled divalent element partition coefficients for anorthite rims and coexisting CAI melt (CMAST), run 224SAM21, compared with data and parameterization for run 2b-2-2 (CMAS) of similar major element composition. D^m_{MgVIII} uncertainty assumed to be 10%; all other error (1 σ) given in parentheses and applies to the last digit shown. $\chi^2 = [(\ln D^{data} - \ln D^{model})/\ln\sigma^{data}]^2$ for each parameterization.

	D^m_{MgVIII}	D^m_{CaO}	D^m_{SrO}	D^m_{BaO}
224SAM21	0.013 (1)	0.728 (4)	1.05 (40)	0.27 (7)
CMAS2b-2-2	0.008 (1)	0.738 (4)	0.92 (4)	0.15 (2)
	D_o	E (GPa)	r_o (Å)	χ^2
224SAM21	1.13	121 (13)	1.223 (4)	2.79
CMAS2b-2-2	1.04	134 (11)	1.209 (2)	6.21

Molar partition coefficients of divalent elements in 224SAM21 are tabulated in Table A4.2, with D^m_{MgVIII} for this composition estimated according to the site occupancy modeling of Section 2.3.3, assuming that several wt. % TiO_2 has little effect on the thermodynamics predicted by the Berman (1983) CMAS melt model and any reoptimization (chapter 3) thereof. Lattice strain parameterizations shown in Table A4.2 were calculated from the partitioning data shown (including D^m_{MgVIII}) and equation (2.1) of chapter 2. Results are compared to values obtained from partitioning observed in

CMAS2b-2, the composition of those studied in chapter 2 most like 224SAM. Since the compositions are not identical in major element contents, the observed variations in D_o, E, and r_o cannot be conclusively attributed to addition of TiO_2. However, the similarities in lattice strain model parameters within analytical uncertainty do suggest that whatever effects TiO_2 may have are likely minor.

A4.2 Anorthite Zoning and Cathodoluminescence Intensity Imaging by SEM

The occurrence of bright cathodoluminescence (CL) with intensity variations resembling compositional zoning in crystals grown from 224SAM melt prompted a reconnaissance investigation into the feasibility of using CL as a quick method of identifying anorthite crystal heterogeneity. CL is known to be a common feature in volcanic and metamorphic feldspars (Gotze et al., 2000; Marshall, 1988), so greater understanding of CL mechanisms potentially provide further insight into crystal growth in natural systems.

Trace constituents may serve to activate, enhance, or quench mineral luminescence in response to electron beam interactions depending on their electronic structure, location in a mineral, and concentration (Marshall, 1988). Sources of CL in materials are difficult to isolate when abundances of activators can be well below detection limits of many *in situ* analytical techniques, and thus many CL phenomena remain poorly understood. However, this sensitivity to structural defects and low abundances of trace elements in crystals make CL a powerful tool in recognizing complex zonation patterns that offer unique records of magma chamber dynamics and

mixing inaccessible by other analytical methods (e.g., Slaby and Gotze, 2004; Stirling et al., 1999; Vanko and Laverne, 1998). Specific wavelengths of CL emissions have been attributed to the presence of specific cations and valence states, though observations here are restricted to intensity. The Caltech LEO 1550 VP FE-SEM currently does not have CL emission wavelength imaging capabilities, but some variations in CL intensity are detectable. Images in Figures A4.1 through A4.5 were obtained by removing the electron detector (EBSD) and observing light emitted in response to a 14-15 kV accelerating voltage with the variable pressure secondary electron detector (VPSE) signal.

Figure A4.1 (a) and (b) show that in addition to emitting striking CL intensity relative to the surrounding melt, anorthite crystals in sample 224SAM21 also contain internal light intensity variations. A 2-D polygonal point grid across a crystal containing an especially bright zone was analyzed for major and trace elements at low (25 nA) beam current on an electron microprobe, with the standards and operating conditions described in Section 2.2.4. Compositional maps (c) and (d) and the correlation plot Figure A4.2 (a) indicate that the region of elevated CL intensity corresponds to an increase in MgO content and decrease in Al_2O_3, suggesting the substitution mechanism,

$$Mg^{2+} + Si^{4+} = 2Al^{3+},$$

where Ti^{4+} would also participate in place of Si^{4+}.

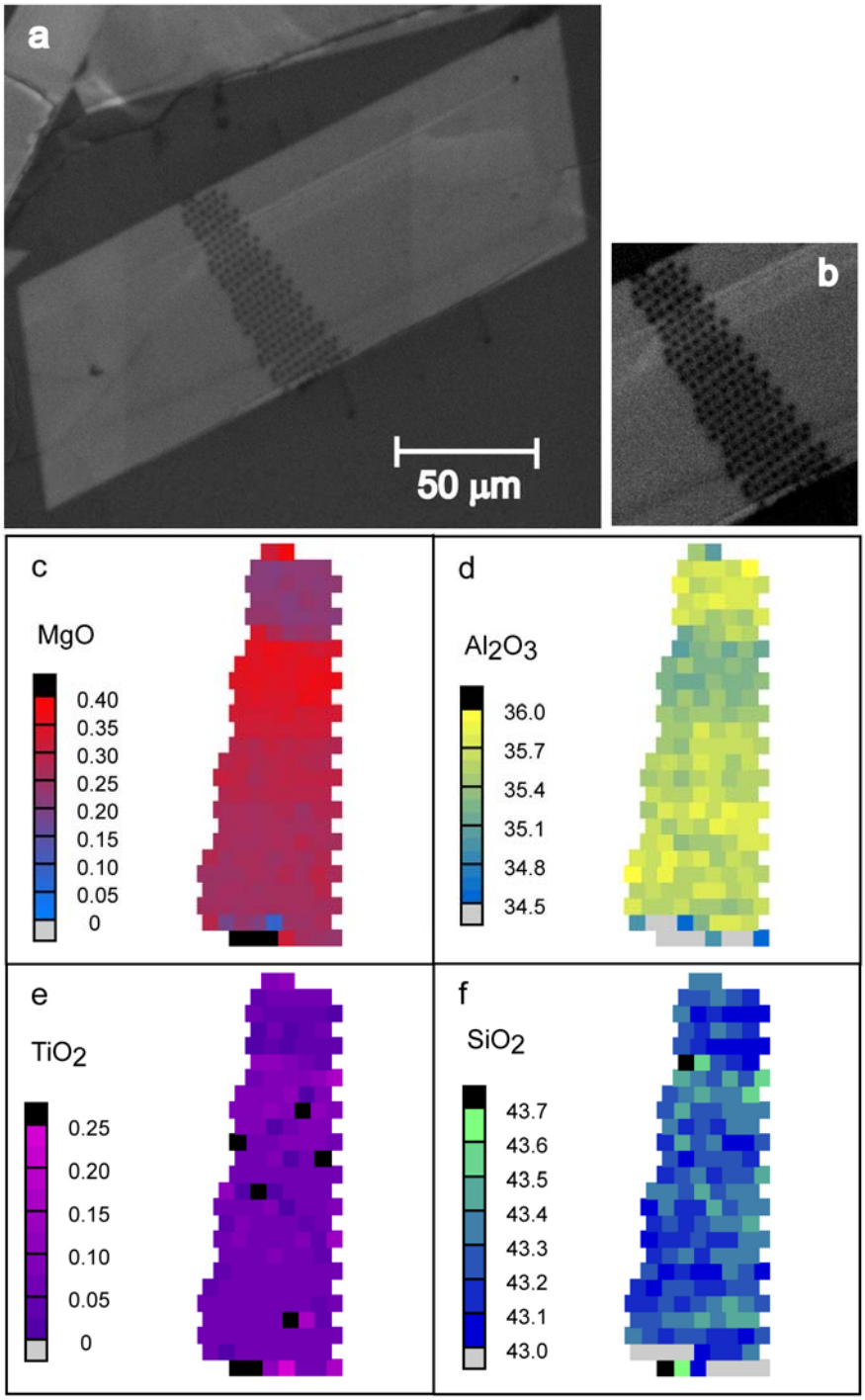

Figure A4.1. (a) SEM cathodoluminescence intensity variations in representative anorthite lath of 224SAM21. (b) Zoom in on band on greater CL intensity and EMP beam burn marks on carbon coat. (c) MgO content (wt. %) of 2-D polygonal grid represented by beam spots of (a) and (b). (d) Al_2O_3 (wt. %), (e) TiO_2 (wt. %), and (f) SiO_2 (wt. %).

Visual inspection of Figure A4.1 (e) and (f) suggests a faint elevation of both TiO_2 and SiO_2 in the region of the crystal corresponding to elevated Mg content. Increased TiO_2 as a function of MgO becomes more apparent in Figure A4.2 (c), though evidence of a SiO_2-MgO correlation from the data shown in Figure A4.2 (b) is equivocal. Likewise, plots (d), (e), and (f) show little MgO dependence on Na_2O, CaO, or BaO in the anorthite crystal.

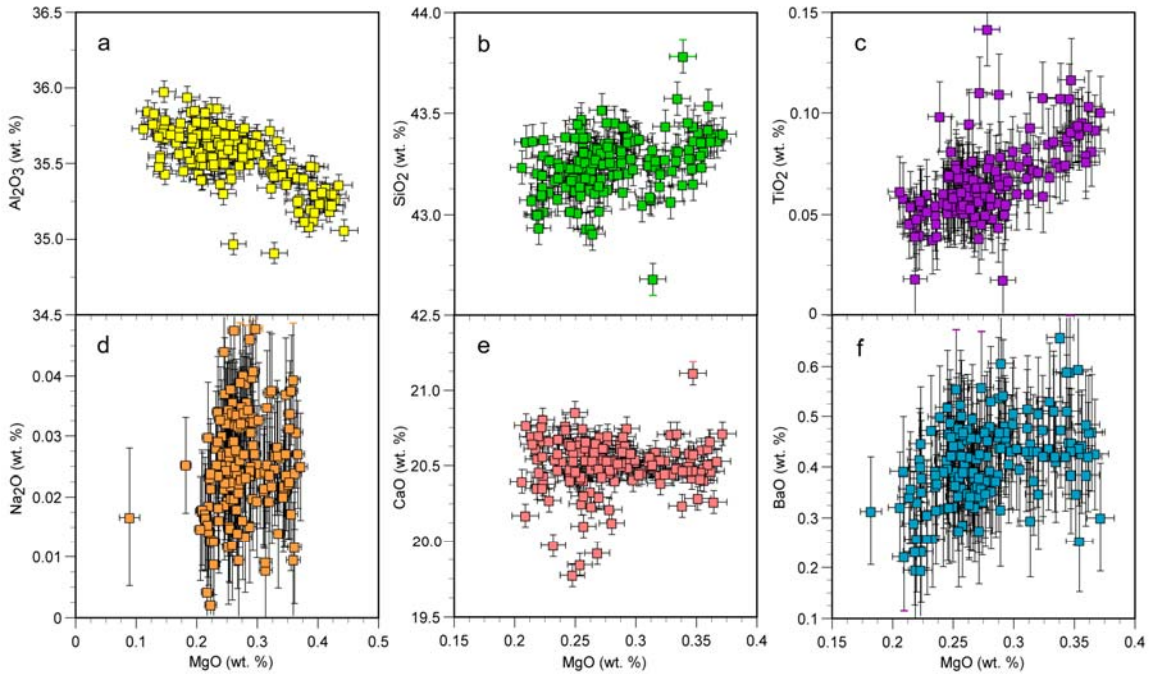

Figure A4.2. Anorthite lath of 224SAM21 correlation plots against MgO content (wt. %) for (a) Al_2O_3, (b) SiO_2, (c) TiO_2, (d) Na_2O, (e) CaO, and (f) BaO. Analytical error for each analysis is 1 σ.

Several controlled cooling experiments using major element compositions 224SAM and CMAS2-2 doped with different concentrations of trace and minor elements were conducted to further investigate sources of CL in synthetic anorthites and explore whether CL could be used as a zoning marker for divalent element heterogeneity in

studies of anorthite like that discussed in chapter 2. Doping concentrations for each run are given in Table A4.3, though sample products were only inspected visually by SEM and no concentrations have been confirmed by quantitative analysis.

Synthetic anorthites grown from CMAS melts doped with Sr and Ba emit no cathodoluminescence, and this is true for both CMAS1 samples (Figure A4.5abc) as well as CMAS2 compositions (not shown). This narrows the potential source of CL emissions from the 224SAM composition to the presence of Ti^{4+} and/or Eu^{3+} under the highly oxidizing (air) atmospheric conditions of this study or possible structural defects associated with their substitution into the crystal.

Table A4.3. Summary table of cathodoluminescence reconnaissance study controlled cooling experiments, with run labels indicating major element starting material compositions. Approximate doping concentrations of trace elements and whether or not anorthite crystals displayed any CL intensity are also listed.

Run label	Trace/minor element doping concentrations	CL?
224SAM-Eu	~2 wt. % TiO_2, 750 ppm Eu, 750 ppm Sr, 1500 ppm Ba	Yes
CMAS2-2-Ti	1000 ppm Ti	No
CMAS2-2-Eu	750 ppm Eu	No
CMAS2-2-Mn	1000 ppm Mn, 1000 ppm Sr, 1500 ppm Ba	No
CMAS2-2-Ge	~2 wt. % GeO_2	No

Previous observations of CL in synthetic anorthites grown from composition 224 melts have found that luminescence intensity correlates with decreases in MgO and Na_2O abundance, with no apparent relationship to TiO_2 content (Steele et al., 1997). Small differences in anorthite Na_2O content in CMAS1 run products ($An_{99.7}$, $An_{95.8}$, $An_{95.8}$ for runs 1-1-2, 1-3-9, and 1-6-8) do not appear to generate any CL variations, as shown in

Figure A4.5, though the CMAS1 abundances span the range of sodium contamination reported in Steele et al. (1997).

Steele et al. (1997) also inspected run products ES55 and ES60, which had oxygen fugacities of C/CO ($\sim 10^{-19}$) and air, respectively, from Peters et al. (1995) with identical results, suggesting the source of CL in those samples was unrelated to any particular cation valence state. They found these observations consistent with those of an Allende anorthite study by Hutcheon et al. (1978), and Vanko and Laverne (1998) also noticed lower CL intensity with higher MgO contents in MOR plagioclases. These works lie in stark contrast to the results of this study, as documented in Figures A4.1 and A4.2, which show CL intensity increasing with MgO and TiO_2 content.

The primary difference between the Steele et al. (1997)/Peters et al. (1995) compositions and that of this study is that 224SAM was doped with ~750 ppm Eu. Eu in open air experiments is likely to be mostly trivalent and assuming $D_{Eu} \sim 0.1$ (Bindeman et al., 1998), Eu contents of anorthite here were likely on the order of 50-100 ppm. Distinctive CL in synthetic anorthite doped with ~200 ppmw Eu^{2+} has been observed (Mariano and Ring, 1975), but doping the initial melt composition CMAS2-2 with ~750 ppm Eu^{3+} produced no CL in anorthite (Figure A4.3a). CMAS2-2 was chosen for doping because it is the closest CMAS analogue of composition 224 available from the CMAS1 and CMAS2 materials. Although some reports attribute an intense blue CL emission to the presence of Ti^{4+} (e.g. Mariano et al., 1973; Marshall, 1988; Stirling et al., 1999), spiking an aliquot of CMAS2-2 with 1000 ppm Ti did not result in growing luminescent anorthites, at least within the ability of the SEM to detect CL (see Figure A4.3b). The concentration of Ti in CMAS2-2-Ti anorthite may have been too low to produce

detectable CL, since D_{Ti} anorthite/melt values (Peters et al., 1995) suggest that these anorthites likely contained ~50 ppm Ti and previous work has found that 0.05–0.1 wt. % TiO_2 was necessary to produce CL in feldspars (Mariano et al., 1973).

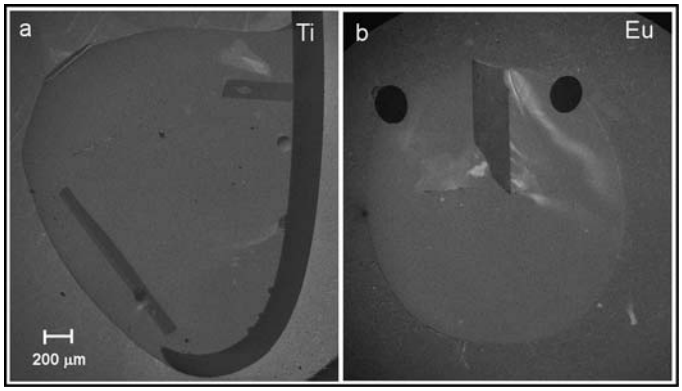

Figure A4.3. SEM CL intensity images of (a) CMAS2-2-Ti, and (b) CMAS2-2-Eu. Bright wisps are likely surface contamination features. Anorthite crystals are dark gray and semi-rectangular, while Pt wire appears as black hook (a) and ovals (b).

Since manganese is well known for generating a distinctive green/yellow CL in plagioclase (e.g. Geake et al., 1973; Gotze et al., 2000; Mariano et al., 1973; Slaby and Gotze, 2004; Stirling et al., 1999; Telfer and Walker, 1978), another aliquot of CMAS2-2 was spiked with 1000 ppm Mn and run under reducing Ar gas flow, though exact f_{O2} was not monitored. Although Mn^{2+} CL activation occurs at concentrations below 20 ppm (Gotze, 1998; Gotze et al., 2000), no CL was detected in anorthites of run CMAS2-2-Mn (Figure A4.4b).

Some workers have speculated that a wide blue band of CL in feldspars, and common to silicates in general, results from an intrinsic luminescence produced by structural defects (Geake et al., 1973; Marshall, 1988). Pack and Palme (2003) observed ubiquitous CL in synthetic forsterites grown from both undoped CMAS and CMAS+Ti compositions, with intensity correlating with increased TiO_2 in the Ti-bearing systems

and Al_2O_3 content of forsterite in the CMAS compositions. An EPR (electron paramagnetic resonance) investigation of feldspars observed that high anorthite content seems to prevent formation of Al-O^--Al defect centers (Speit and Lehmann, 1982), which are attributed to the 450-480 nm CL emission band (Gotze et al., 2000). The fact that anorthites of this study have a pure end-member composition and, except for 224SAM anorthites, show no CL would be consistent with a lack of CL-producing Al^{3+} defects.

"Si-O^-…-M^{2+}" defects associated with a 500–510 nm band could also be a candidate for producing the 224SAM CL, since this defect is characterized by an oxygen hole next to a divalent ion in an adjacent tetrahedral site (Speit and Lehmann, 1982) and CL in this study is correlated with Mg content. The bulk of Mg in plagioclase likely resides on the tetrahedral site (Longhi et al., 1976; Miller et al., 2006; Peters et al., 1995), though this cannot be the primary source of CL in these experiments when tetrahedral Mg occurs in all the anorthites of the 224SAM, CMAS1, CMAS2, and CMAS2b compositions but only 224SAM produces CL. CMAS2 melt compositions were also spiked with ~500 ppm Be, another divalent element populating anorthite T sites, and those anorthites exhibited no CL.

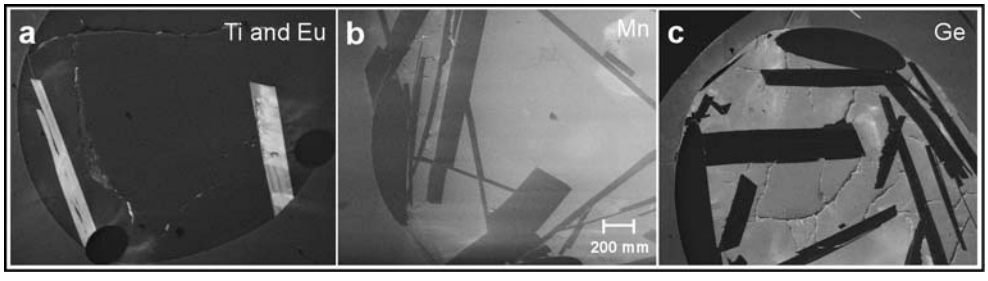

Figure A4.4. SEM-CL images of (a) striking intensity of anorthite crystals from 224SAM-Eu-1, (b) no CL intensity in CMAS2-2-Mn, and (c) no CL intensity in the crystals of CMAS2-2-Ge.

The hypothesis that Ti^{4+} might enhance defect-related luminescence was tested by doping CMAS2-2 with an amount of GeO_2 comparable to the TiO_2 content of 224SAM (~2 wt. %). Since Ge^{4+} has an ionic radius similar to that of Ti^{4+} (0.39 and 0.42 Å, respectively) and the same valence state, it seemed reasonable that the partition coefficients and structural positions of these ions would be similar in anorthite. As seen in Figure A4.4c, the Ge-doped crystals emit no CL. Furthermore, excess silica in the anorthite structure also appears to have no role in generating CL emissions (Figure A4.5). The source(s) of CL in the 224SAM anorthite crystals remain unknown.

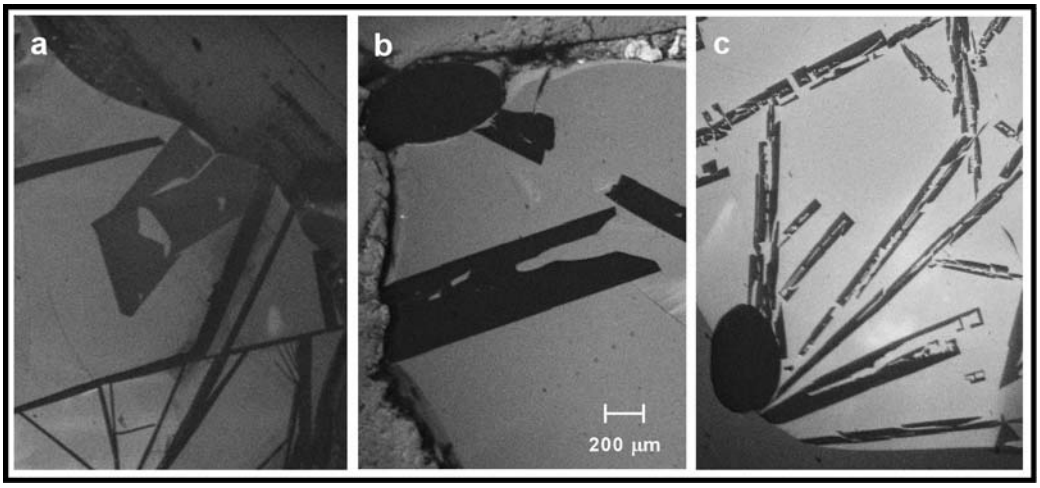

Figure A4.5. SEM CL intensity images comparing the effect varying extents of structural excess silica in anorthite on cathodoluminescence intensity. (a) CMAS1-1-6, (b) CMAS1-3-9, and (c) CMAS1-6-8.